sustainability

MDPI

Article

An Integrated GIS and Explainable AI Framework for Climate-Resilient Municipal Pavement Management: Quantifying the Influence of Maintenance, Hydrological, and Environmental Factors on Pavement Condition Index (PCI)

Shishir Bhusal [1], Nicholas Brake [1,*], Arip S. Nur [1], Mahdi Feizbahr [1], Hossein Hariri Asli [1] and Muna Kandel [2]

[1] Department of Civil and Environmental Engineering, Lamar University, Beaumont, TX 77710, USA; sbhusal1@lamar.edu (S.B.); anur@lamar.edu (A.S.N.); mfeizbahr@lamar.edu (M.F.); hhaririasli@lamar.edu (H.H.A.)
[2] Department of Computer Science, Lamar University, Beaumont, TX 77710, USA; mkandel1@lamar.edu
* Correspondence: nbrake@lamar.edu

Abstract

Accurate prediction of pavement performance is essential for sustainable pavement management, especially in flood-prone regions where environmental stressors accelerate deterioration. This study develops a machine learning-based comparative framework to evaluate the contributions of baseline pavement condition, maintenance and rehabilitation (M&R) activities, and environmental exposure to predicting changes in Pavement Condition Index (ΔPCI) across 11,214 matched pavement segments in Southeast Texas from 2019 to 2023. Three nested modeling scenarios were evaluated using Linear Regression, Random Forest, and XGBoost, with performance evaluated using R^2, MAE, and RMSE. Baseline variables alone showed limited predictive capability, whereas adding M&R history produced the largest improvement. Environmental and flood-related variables provided further gains, particularly for nonlinear ensemble models. XGBoost achieved the highest predictive performance in the fully integrated scenario (R^2 = 0.65, MAE = 10.63, RMSE = 14.02). SHAP analysis identified SDI2019 and PCI2019 as the strongest predictors, while selected M&R and environmental variables also contributed meaningfully. The findings demonstrate that integrating treatment history and environmental exposure substantially improves pavement performance prediction and supports more sustainable, climate-resilient pavement management and helps agencies prioritize maintenance and allocate resources more effectively.

Keywords: pavement; machine learning; maintenance and rehabilitation; Pavement Condition Index (PCI); flood-prone infrastructure; environmental exposure; pavement management

Check for updates

Academic Editor: Piergiorgio Tataranni

Received: 8 May 2026
Revised: 15 June 2026
Accepted: 23 June 2026
Published: 26 June 2026

Copyright: © 2026 by the authors. Licensee MDPI, Basel, Switzerland. This article is an open access article distributed under the terms and conditions of the Creative Commons Attribution (CC BY) license.

1. Introduction

Pavement infrastructure is a critical component of transportation systems because it directly affects roadway safety, mobility, serviceability, and economic performance. To support efficient maintenance planning and resource allocation, pavement agencies commonly rely on condition indicators such as the Pavement Condition Index (PCI) and the International Roughness Index (IRI), which are widely used within pavement management

systems (PMS) to monitor network condition and prioritize maintenance and rehabilitation (M&R) actions [1–4]. As roadway networks continue to age and environmental stressors become more severe, accurate prediction of pavement performance has become increasingly important for sustainable infrastructure management.

Pavement deterioration is governed by the combined influence of structural condition, traffic loading, environmental exposure, and maintenance history. Previous studies have shown that traffic and structural characteristics strongly influence fatigue, rutting, and surface distress progression, while climatic variables such as precipitation, temperature variation, and moisture exposure can accelerate deterioration processes [5–8]. In flood-prone regions, repeated inundation can weaken pavement support layers, reduce structural stability, and intensify deterioration, particularly in low-lying and poorly drained areas [9–13]. Ground deformation and related geotechnical instability may further aggravate pavement vulnerability, especially in regions subject to frequent hydrologic stress [14–16].

Conventional pavement performance models are often based on deterministic or regression-based approaches using historical condition indicators. Although such methods are useful for network-level planning, they may not fully capture nonlinear relationships and interaction effects among baseline pavement conditions, treatment history, and environmental stressors. Recent advances in machine learning (ML) have improved pavement performance prediction by enabling flexible modeling of high-dimensional and nonlinear data structures [17,18]. Ensemble methods such as Random Forest and Extreme Gradient Boosting (XGBoost) have shown promising performance in pavement condition prediction and infrastructure deterioration modeling [17–21].

Although machine learning has been increasingly applied to pavement condition prediction, several gaps remain in the context of sustainable and climate-resilient pavement management. Many previous studies focus on predicting static pavement condition indicators, such as PCI or IRI, rather than modeling performance change over time. In addition, maintenance history is often represented in simplified form [22,23], and environmental stressors are frequently evaluated separately from treatment effects [16,24–26]. These limitations make it difficult for agencies to understand how existing pavement conditions, M&R activities, and climate-related exposure jointly influence pavement performance changes at the network level.

To address these gaps, this study develops a comparative machine-learning framework to predict pavement performance change in Southeast Texas using ΔPCI as the response variable. Unlike prior ML-based pavement studies that modeled static conditions such as point-in-time PCI estimation [20,21] or IRI prediction at a single inspection cycle [6,19]—this study uses ΔPCI as the response variable. Modeling ΔPCI rather than static PCI enables the analysis to focus on actual performance change over time, supports direct evaluation of deterioration trends and M&R associations at the network level, and reduces the bias that arises when treating condition measurements from different inspection years as independent static observations. The framework evaluates three nested feature scenarios: baseline pavement and roadway variables, baseline variables plus M&R history, and a fully integrated model that also includes environmental and flood-related variables. This structure allows the incremental contribution of M&R and environmental exposure to be quantified and compared. In addition, SHAP analysis is used to interpret model-based feature contributions and provide explainable insights for pavement management decision-making.

The study contributes to sustainable pavement management in three main ways. First, it provides a matched segment ΔPCI modeling framework for evaluating pavement performance change across a real-world urban road network. Second, it quantifies how treatment history and environmental exposure improve prediction beyond baseline pavement con-

dition and roadway classification variables. Third, it interprets the relative importance of baseline, M&R, and environmental factors using SHAP, supporting more transparent prioritization of maintenance actions in flood-vulnerable regions. These contributions can assist transportation agencies in allocating limited maintenance resources more efficiently, identifying climate-sensitive pavement segments, and developing long-term strategies for resilient and sustainable infrastructure management. In contrast to conventional PMS approaches that rely on deterministic deterioration curves or single-variable regression models, the proposed framework uses ensemble machine learning with SHAP-based interpretation to simultaneously capture the nonlinear and interacting effects of baseline condition, treatment history, and environmental exposure, providing a more flexible and explainable basis for network-level pavement performance forecasting. Accordingly, the objectives of this study are:

- to compare the predictive performance of Linear Regression, Random Forest, and XGBoost for estimating pavement performance change (ΔPCI)
- to quantify the incremental contribution of M&R and environmental variables beyond baseline pavement and roadway classification features
- to interpret the influence of key variables using SHAP-based model explanation
- to demonstrate how integrated pavement, maintenance, and environmental data can support sustainable and climate-resilient pavement management in flood-prone urban networks.

2. Study Area and Data Description

2.1. Study Area

The study area is in Southeast Texas, United States, with a primary focus on Jefferson County and the City of Beaumont. This region experiences a humid subtropical climate and is highly susceptible to extreme weather events such as heavy rainfall, flooding, and hurricanes. The combination of low-lying terrain, proximity to the Gulf of Mexico, and dense urban roadway networks makes pavement infrastructure in this area particularly vulnerable to moisture-related deterioration mechanisms.

Figure 1 illustrates the spatial extent of the study area and the extracted road network of Beaumont used for the analysis. Frequent flooding and variable climatic conditions accelerate pavement degradation processes, including roughness progression, surface distress, and structural weakening. As a result, Southeast Texas provides a representative case for evaluating pavement performance under combined structural, operational, and environmental stressors.

2.2. Data Sources and Integration

This study utilizes an integrated multi-source dataset derived from publicly available and previously published resources, with detailed data collection procedures documented in Asli, Brake [24]. Pavement condition data, including segment-level Pavement Condition Index (PCI) and International Roughness Index (IRI), were obtained from the City of Beaumont pavement management system (PMS) using a Laser Road Surface Tester following ASTM D6433-11 standards, along with pavement type, functional classification, and geometric attributes.

Each roadway segment was identified using a unique GIS identifier (GISID), which served as the primary key for linking pavement condition records, spatial attributes, M&R information, and environmental variables across datasets. In this study, a roadway segment refers to a GISID-based pavement management unit defined by its street location and boundaries, including the on-street name and the corresponding from-street and to-street reference points. Therefore, the segment definition follows the City of Beaumont PMS and

GIS inventory structure and represents a block-level or management-level roadway unit rather than a fixed-length pavement sample.

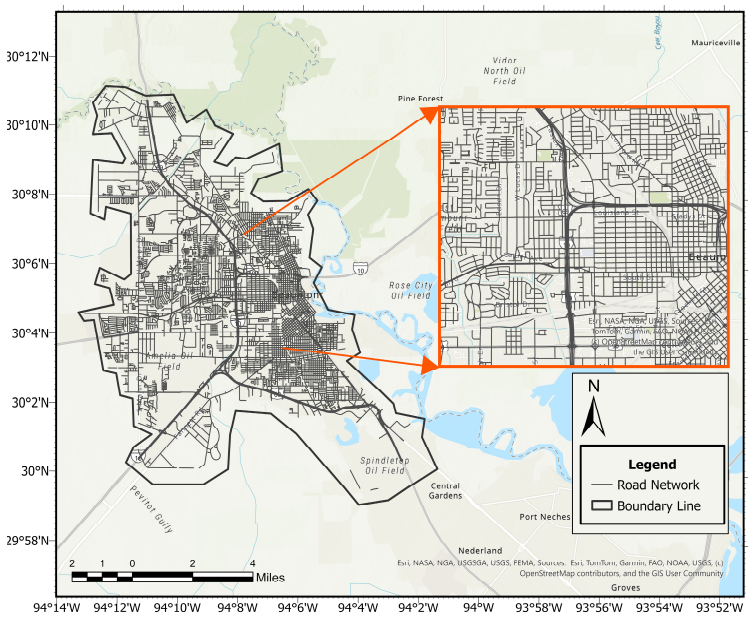


Figure 1. The study area of Beaumont, Texas, is located in Jefferson County, Southeast Texas.

The 2019 and 2023 pavement inspection datasets were matched using GISID so that pavement performance change could be calculated for the same roadway segment across the two inspection years. The raw 2019 inspection dataset contained 11,889 unique GISID records, and the raw 2023 inspection dataset contained 13,974 unique GISID records. GISID-based matching identified 11,783 common roadway segments with inspection records in both years. During the final cleaning and feature-integration stage, segments with inconsistent records or incomplete required modeling attributes were removed, resulting in a final model-ready dataset of 11,214 matched pavement segments. Therefore, the 11,214 records used in this study do not represent cumulative observations across years; instead, each row corresponds to the same roadway segment observed in both 2019 and 2023.

Environmental and climatic variables were integrated from PRISM, NOAA/National Weather Service datasets, Sentinel-1 radar-based flood data, and previously developed hydrologic and geospatial model outputs. Climatic variables, including precipitation and temperature, were processed at a monthly resolution and spatially localized to the segmented road network using ArcGIS Pro 3.5.0. Geospatial operations such as inverse distance weighting (IDW) interpolation, raster reclassification, spatial joins, and zonal statistics were used to assign segment-level climate and environmental values to GISID-linked roadway segments [24]. Flood-related and terrain variables, including flood frequency, inundation depth, flood susceptibility index [27], topographic control index (TCI) [28], and ground deformation, were derived through remote sensing, hydrologic modeling, and geospatial processing as described in Asli, Brake [24]. All datasets were spatially aligned and merged at the segment level to create a unified dataset suitable for machine learning analysis.

2.3. Dataset Overview and Feature Groups

The final dataset consists of 11,214 matched pavement segments with corresponding inspection records in both 2019 and 2023. Pavement performance change was quantified using the difference in Pavement Condition Index between the two observation years:

$$\Delta PCI = PCI_{2023} - PCI_{2019} \quad (1)$$

where positive ΔPCI values indicate improvement in pavement condition, and negative values indicate deterioration over the study period. Using ΔPCI enables direct representation of changes in pavement performance for the same roadway segment, supporting evaluation of deterioration trends, M&R associations, and environmental exposure effects, while reducing bias associated with static condition modeling. Input variables were organized into three feature groups: (i) baseline pavement condition and geometric features, (ii) maintenance and rehabilitation (M&R) activities, and (iii) environmental and flood-related variables. This structured grouping supports systematic evaluation of the incremental contribution of each feature group to pavement performance prediction, consistent with the comparative modeling framework adopted in this study.

3. Materials and Methods

3.1. Modeling Workflow

The overall methodological framework consisted of data acquisition, integration, preprocessing, feature grouping, model development, performance evaluation, and model interpretation. This workflow enables a structured comparison of baseline, M&R-enhanced, and environmentally enriched models, supporting evaluation of their relative contributions to ΔPCI prediction and directly addressing the research gap related to modeling pavement performance change over time. Figure 2 illustrates the workflow of the comparative machine-learning framework adopted in this study.

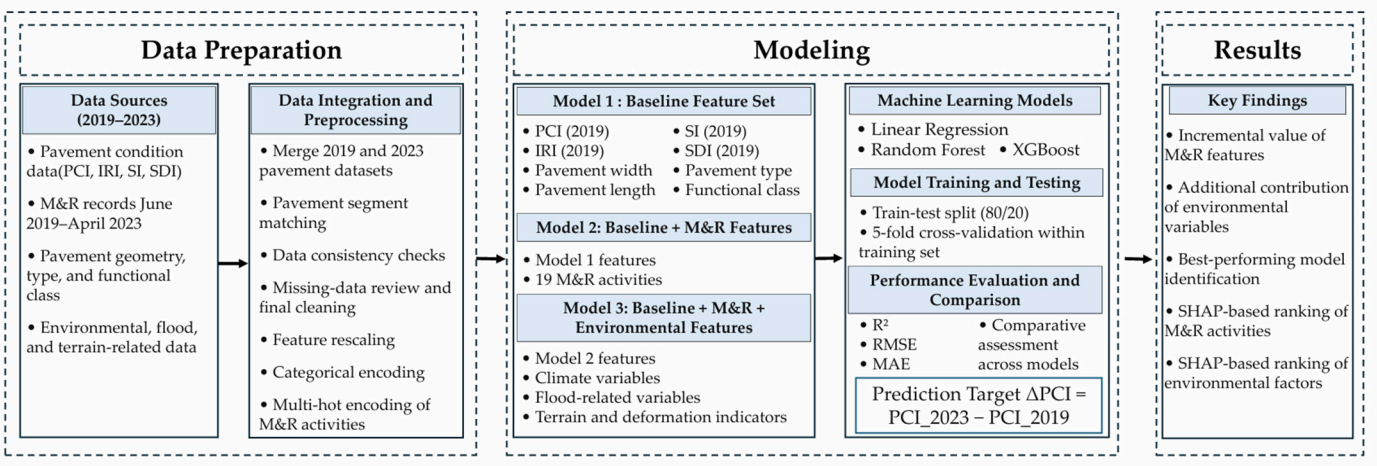


Figure 2. Workflow of the comparative machine-learning framework for ΔPCI prediction.

3.2. Feature Grouping and Modeling Scenarios

We evaluate three nested scenarios: Model 1 (Baseline), which includes pavement and roadway descriptors; Model 2 (Baseline + M&R), which adds maintenance and rehabilitation indicators; and Model 3 (Baseline + M&R + Environmental), which adds environmental and flood-related variables. This structure enabled systematic comparison of how treatment history and environmental exposure improved prediction beyond the baseline pavement and roadway descriptors commonly used in pavement management practice [1–4].

3.2.1. Baseline Feature Set (Model 1)

Model 1 represented the baseline pavement performance prediction scenario. It included the core pavement condition, geometric, and classification variables available at the beginning of the analysis period:

- Pavement Condition Index in 2019 (PCI2019, dimensionless index, 0–100 scale)
- International Roughness Index in 2019 (IRI2019, mm/m)
- Pavement width (ft)
- Pavement length (ft)
- Structural Index in 2019 (SI2019, dimensionless categorical index: 30 = weak, 60 = moderate, 80 = strong)
- Surface Distress Index in 2019 (SDI2019, dimensionless index)
- Pavement type (categorical, code: 1 = asphalt, 2 = concrete, 3 = composite)
- Functional class (categorical, code: 1 = arterial, 2 = collector, 3 = local)

This feature set served as the reference scenario and reflected the core structural, condition, and roadway classification information commonly available in pavement management systems for performance assessment, budgeting, and prioritization of interventions [1–4].

3.2.2. Maintenance and Rehabilitation (M&R) Variables

Maintenance and rehabilitation (M&R) activities were incorporated as key explanatory variables to capture treatment history associations with pavement performance change. A total of 19 distinct M&R activities were identified from the dataset covering the period from June 2019 to April 2023. Each activity was encoded using a binary (Boolean) representation, where a value of TRUE indicates that a specific treatment was applied to a pavement segment during the observation period, and FALSE indicates no application. This multi-hot encoding approach allows multiple treatments to be represented simultaneously for a single segment.

The available M&R dataset identified whether a treatment category was recorded for each segment during the June 2019–April 2023 observation period. However, the dataset provided by the City of Beaumont did not include consistently available treatment timing, sequencing, construction quality, or treatment dosage information for all matched segments. Therefore, M&R activities were represented as binary indicators in the modeling framework. This encoding captures whether each treatment type was associated with a segment during the analysis period, but it does not model treatment age, treatment order, or duration of post-treatment exposure. These limitations are considered when interpreting the M&R-related SHAP results and are further discussed in the limitations section. Table 1 provides a detailed description of all M&R activities considered in this study, along with their encoding and functional classification. The inclusion of treatment history in pavement performance modeling is supported by previous work emphasizing that the predictive association between treatment type and performance change depends strongly on the nature of the intervention and the condition of the pavement at the time of application [22,23].

3.2.3. Baseline + Maintenance and Rehabilitation Features (Model 2)

The second modeling scenario extended the baseline feature set by incorporating M&R history. Therefore, Model 2 included all Model 1 variables together with multi-hot encoded indicators representing the 19 distinct M&R activities applied between June 2019 and April 2023. By comparing Model 2 against Model 1, the incremental explanatory value of treatment history could be directly quantified. This comparison is important because pavement performance is influenced not only by baseline condition but also by the type and timing of maintenance interventions and evaluating detailed treatment history can improve understanding of how M&R activities contribute to ΔPCI prediction [5,16,22,24].

Table 1. Maintenance and rehabilitation (M&R) activities, encoding, and functional classification.

M&R Activity	Encoding	Category	Description
ACP Full Depth Reconstruction	Binary (TRUE/FALSE)	Rehabilitation (Structural)	Complete reconstruction of asphalt pavement layers
EM/FWM + Moderate Overlay (2.0–3.0)	Binary (TRUE/FALSE)	Rehabilitation	Milling combined with moderate thickness overlay
EM/FWM + Moderate Overlay (2.0–3.0) + Strctrl Ptch	Binary (TRUE/FALSE)	Rehabilitation	Overlay combined with structural repair
Edge Mill + Thin Overlay (1.5–2.0)	Binary (TRUE/FALSE)	Preventive/Minor Rehabilitation	Edge correction with thin overlay
Edge Mill + Thin Overlay (1.5–2.0) + Strctrl Ptch	Binary (TRUE/FALSE)	Rehabilitation	Edge milling with localized structural repair
FWM + Thick Overlay (>2.0–3.0)	Binary (TRUE/FALSE)	Major Rehabilitation	Thick overlay following milling
FWM + Thick Overlay (>2.0–3.0) + Strctrl Ptch	Binary (TRUE/FALSE)	Major Rehabilitation	Major overlay with structural repair
Micro Surface/Chip Seal	Binary (TRUE/FALSE)	Preventive Maintenance	Surface sealing treatment to extend pavement life
Micro Surface/Chip Seal + Strctrl Ptch	Binary (TRUE/FALSE)	Preventive + Corrective	Surface treatment with localized repair
PCC Extensive Pnl Rplcmnt (<33%) + Grind	Binary (TRUE/FALSE)	Rehabilitation (Concrete)	Large-scale panel replacement and surface grinding
PCC Jnt Rehab & Crk Seal	Binary (TRUE/FALSE)	Preventive Maintenance	Joint and crack sealing for concrete pavements
PCC Localized Rehab	Binary (TRUE/FALSE)	Corrective Maintenance	Localized concrete repair
PCC Localized Rehab + Grind	Binary (TRUE/FALSE)	Corrective Maintenance	Local repair combined with grinding
PCC Moderate Pnl Rplcmnt (<20%) + Grind	Binary (TRUE/FALSE)	Rehabilitation	Moderate panel replacement and grinding
PCC Slight Pnl Rplcmnt (<10%)	Binary (TRUE/FALSE)	Preventive/Minor Rehabilitation	Minor panel replacement
PCC Slight Pnl Rplcmnt (<10%) + Grind	Binary (TRUE/FALSE)	Preventive/Minor Rehabilitation	Minor repair with grinding
Routine Maintenance	Binary (TRUE/FALSE)	Preventive Maintenance	Routine minor maintenance activities
Slurry Seal/Seal Coat	Binary (TRUE/FALSE)	Preventive Maintenance	Surface sealing for protection and durability
Surf Recon + Base Rehab/FWM + Strctrl Ptch + Olay	Binary (TRUE/FALSE)	Major Rehabilitation	Combined structural and surface reconstruction

Note: "ACP" = Asphalt Concrete Pavement; "EM" = Edge milling; "FWM" = Flexible Wear Maintenance; "PCC" = Portland Cement Concrete; "Strctrl Ptch" = Structural Patching; "Olay" = Overlay; "Pnl Rplcmnt" = panel replacement; "Jnt Rehab" = Joint Rehabilitation; "Crk Seal" = crack sealing; "Grind" = Diamond Grinding; "Recon" = Reconstruction; "Rehab" = Rehabilitation. Structural Patching refers to localized repair of deteriorated pavement sections prior to overlay application. All M&R activities were encoded as binary/categorical treatment indicators, where True indicates that the treatment was recorded for a segment and False indicates that it was not recorded.

3.2.4. Baseline + Maintenance and Rehabilitation + Environmental Features (Model 3)

The third modeling scenario integrates baseline pavement attributes, maintenance and rehabilitation information, and environmental and flood-related variables to evaluate the combined influence of structural, operational, and climatic factors on pavement performance. In addition to all variables included in Model 2, Model 3 incorporated the following environmental variables:

- Mean temperature (MeanTemp_avg, °C): Represents cumulative thermal exposure over the observation period. Elevated temperatures accelerate binder oxidation and thermal aging in asphalt pavements, increasing surface cracking and brittleness, while temperature cycling drives repeated expansion and contraction that can widen existing cracks and reduce structural integrity over time [5,7].
- Precipitation (PPT_avg, mm): Represents cumulative moisture exposure. High precipitation increases the likelihood of subsurface saturation, which can reduce subgrade bearing capacity, promote moisture-induced stripping in asphalt layers, and accelerate surface distress, particularly in low-lying and poorly drained pavement segments [5,9].
- Inundation depth (Inundation Depth MEAN, ft): The average depth of floodwater sitting directly on top of the road surface during a flood event, i.e., depth measured by taking the road surface as a reference point. A higher inundation depth will cause pavement damage, including subgrade saturation, reduction in bearing capacity, and accelerated surface distress such as cracking and pothole formation.
- Flood frequency (Frequency of Flooding, count): Number of times a road segment experiences flooding; this reflects how often the pavement is exposed to observable flood events from Sentinel-1 images.
- Flood Speed (ft/s): Velocity of floodwater movement across or near the segment. Higher flow velocities exert greater hydraulic shear stress on the pavement surface and surrounding embankments, which can erode shoulder material, undermine edge support, and weaken the subbase through scouring and particle displacement [9,11].
- Water Elevation (ft): The height of the flood water surface measured from a fixed reference point (such as sea level), not from the road surface. A high-water elevation does not always mean the road is directly flooded—its impact depends on how high the road sits relative to the water surface. If the road is low, high-water elevation leads to deep inundation and severe pavement damage. If the road sits higher than the flood water elevation, the road may escape direct inundation even during a major flood event, experiencing little to no surface flooding despite the surrounding area being severely flooded.
- Flood Susceptibility (dimensionless index): Dimensionless index representing the relative likelihood that an area will flood based on combined geospatial and environmental factors; higher values indicate greater flood vulnerability.
- Topographic Control Index (TCI, dimensionless index): A terrain-based index quantifying the tendency of water to accumulate in topographic depressions and low-gradient zones. Higher TCI values indicate greater runoff concentration and prolonged water retention, which can increase the duration of subgrade saturation and accelerate moisture-related pavement deterioration in low-lying areas [13,28].
- Ground deformation (Deformation, mm): Captures vertical ground surface movement, including subsidence or localized uplift, derived from satellite-based radar (PS-InSAR) measurements. Ground subsidence reduces the uniformity of subgrade support beneath the pavement structure, inducing differential settlement, longitudinal cracking, and accelerated surface distress, particularly in areas of geotechnical instability or groundwater-driven consolidation [14,15].

The environmental variables were derived from monthly climatic data and spatially processed flood, terrain, and deformation datasets. Climatic variables, including precipitation and temperature, were obtained from PRISM and NOAA/National Weather Service sources and localized to the segmented road network using ArcGIS Pro 3.5.0 procedures, including IDW interpolation, raster processing, spatial joins, and zonal statistics. The 72-month environmental data structure refers to two 36-month exposure windows associated with the two inspection years: one 36-month period preceding the 2019 inspection and one 36-month period preceding the 2023 inspection. Monthly values were summarized into segment-level representative variables and linked to each GISID-based roadway segment. Flood-related and terrain variables, including flood frequency, inundation depth, flood susceptibility, topographic control index, and ground deformation, were similarly assigned to roadway segments using geospatial overlay and zonal/statistical aggregation procedures. Therefore, environmental variables in this study represent segment-level exposure indicators rather than monthly time-series inputs used directly in the machine learning models. These variables were included to capture climatic, flood-related, terrain, and deformation conditions affecting pavement performance in Southeast Texas, USA. Prior studies have shown that flooding, inundation, terrain-driven drainage behavior, and ground instability can accelerate pavement deterioration, particularly in low-lying and climate-vulnerable regions [9,14,25,29,30].

3.3. Data Preprocessing

Prior to model development, the 2019 and 2023 pavement inspection datasets were merged and processed to produce a unified model-ready dataset. Segment matching was performed using GISID to ensure that observations from the two inspection years corresponded to the same roadway units. As described in Section 2.2, GISID-based matching first identified 11,783 common roadway segments, and the final cleaning and feature-integration process resulted in 11,214 matched pavement segments for modeling.

After matching, duplicate records, inconsistent entries, and segments with incomplete required modeling attributes were removed. Missing data patterns were reviewed before model development. The key pavement condition and geometric variables used in the modeling process, including GISID, pavement width, pavement length, IRI, SDI, SI, and PCI, contained complete records in the retained dataset. The high number of blank entries in the original M&R field reflected segments with no recorded maintenance or rehabilitation activity during the June 2019–April 2023 observation period, rather than missing pavement condition data. These no-treatment cases were encoded as 0 across all M&R binary indicator variables. After cleaning and feature integration, the final model-ready dataset contained no missing values across the variables used for model training; therefore, the missingness rate for all retained modeling variables was 0%.

Median imputation was included in the preprocessing pipeline as a precautionary step for numerical features prior to model training. However, because the final retained modeling dataset contained no missing values, the imputer was invoked but did not replace any values. Thus, missing-value handling in the final analysis was effectively addressed through data cleaning, exclusion of incomplete required records, and complete-case model preparation rather than active numerical imputation. For model preparation, categorical variables, including pavement type and functional class, were encoded prior to model training. M&R activities were transformed using multi-hot encoding (Section 3.2.2 and Table 1), so that each treatment type was represented by a separate binary indicator. Numerical features were rescaled to improve consistency across variables measured in different units and ranges.

Several potentially important pavement performance predictors, including pavement age, structural layer thickness, and traffic loading, were not included because these variables were not available in the City of Beaumont, Texas, USA dataset for all matched segments used in this study. Their absence may partly explain the limited predictive capability of the baseline model and is acknowledged as a limitation and future research direction. This preprocessing workflow enabled the integrated use of pavement condition, roadway, treatment, and environmental variables in a common machine-learning framework [17–19,31].

3.4. Machine Learning Models

Three regression-based models were implemented to predict ΔPCI. These models were selected to allow a structured comparison between a conventional linear baseline and two ensemble-based nonlinear methods that have been widely applied in pavement and infrastructure performance modeling. Although deep learning approaches have also shown promise in pavement prediction, this study prioritized interpretable and high-performing models that are well-suited to structured segment-level tabular data.

3.4.1. Linear Regression

Linear Regression was used as a baseline statistical model to establish a reference level of predictive performance. Although limited in its ability to capture nonlinear relationships, Linear Regression provides interpretability and serves as a benchmark for evaluating more advanced models.

3.4.2. Random Forest Regression

Random Forest (RF) is an ensemble learning algorithm that constructs multiple decision trees using bootstrap samples of the training data and aggregates their predictions through averaging. This approach can capture nonlinear relationships and complex feature interactions while remaining robust to multicollinearity, noise, and outliers. Random Forest has been successfully applied to pavement and roughness prediction problems because it handles heterogeneous tabular inputs effectively and can model nonlinear deterioration processes [17,19].

3.4.3. Extreme Gradient Boosting (XGBoost)

Extreme Gradient Boosting (XGBoost) is a gradient-boosting algorithm that builds decision trees sequentially, where each tree is trained to minimize the residual error of the previous iteration. XGBoost incorporates regularization, subsampling, and efficient optimization strategies that improve predictive accuracy and computational performance. The algorithm has demonstrated strong performance in structured pavement and infrastructure datasets and is particularly well suited for modeling nonlinear and interaction-driven systems [18,31]. In this study, XGBoost was also selected as the primary model for SHAP-based interpretation because of its superior performance in the final comparative analysis.

3.5. Model Training and Evaluation

The dataset of 11,214 pavement segments was randomly divided into training and testing subsets using an 80/20 split, where the training data were used for model development and hyperparameter tuning, and the testing data were reserved as an independent hold-out set for evaluating generalization performance. A five-fold cross-validation procedure was applied exclusively within the training dataset, in which the data were partitioned into five subsets, with four used for training and one for validation in each iteration. This process was repeated five times to ensure that each subset served as the validation set once, enabling robust hyperparameter selection and assessment of model stability while pre-

venting information leakage. After finalizing model configurations, models were retrained on the full training dataset and evaluated on the testing dataset. Learning curve analysis was conducted using the XGBoost model to assess convergence behavior and the effect of training sample size on prediction accuracy. Model performance was evaluated using three regression metrics: the coefficient of determination (R^2), which measures the proportion of variance in ΔPCI explained by the model; the root mean square error (RMSE), which quantifies the average magnitude of prediction error; and the mean absolute error (MAE), which represents the average absolute difference between predicted and observed values.

3.6. Hyperparameter Selection

Hyperparameters for the Random Forest and XGBoost models were selected through systematic tuning using cross-validation and guided by prior literature to balance predictive performance and computational efficiency. Preliminary tuning experiments were conducted to identify suitable parameter ranges while minimizing overfitting and ensuring stable model performance. The final models were trained using fixed hyperparameter values selected from the tuning process to ensure reproducibility and consistency of results. The final hyperparameter settings used in this study are summarized in Table 2.

Table 2. Final hyperparameters used for machine learning models.

Model	Hyperparameter	Final Value
Random Forest	Number of trees (n_estimators)	500
Random Forest	Maximum tree depth (max_depth)	None
Random Forest	Minimum samples per leaf (min_samples_leaf)	1
Random Forest	Features considered at each split (max_features)	sqrt
Random Forest	Random seed	42
XGBoost	Number of boosting iterations (n_estimators)	500
XGBoost	Maximum tree depth (max_depth)	8
XGBoost	Learning rate (learning_rate)	0.03
XGBoost	Subsample ratio (subsample)	0.7
XGBoost	Feature subsample ratio (colsample_bytree)	0.7
XGBoost	Objective function	reg:squarederror
XGBoost	Random seed	42

4. Results

4.1. Baseline Model Results (Model 1)

In this configuration, the models were trained using baseline pavement condition, geometric, and roadway classification variables. The performance results for the baseline model configuration are presented in Table 3.

Table 3. Performance of models using baseline pavement and roadway classification features.

Algorithm	R^2	MAE	RMSE
Linear Regression	0.24	15.94	20.57
Random Forest	**0.35**	**14.45**	**19.03**
XGBoost	0.34	14.43	19.14

Note: Bold values indicate the best performance metric in each column.

The baseline models provided limited predictive capability, with test R^2 values ranging from 0.24 to 0.35. Among the three algorithms, Random Forest achieved the highest baseline performance (R^2 = 0.35), followed closely by XGBoost (R^2 = 0.34), while Linear Regression performed the weakest (R^2 = 0.24). The comparatively high MAE and RMSE values indicate that baseline pavement and roadway descriptors alone do not fully explain

pavement performance change over the study period. These findings suggest that nonlinear relationships are already present in the baseline feature space, but additional explanatory information is required for stronger predictive performance.

4.2. Impact of Maintenance and Rehabilitation Features (Model 2)

Model 2 extended the baseline feature set by incorporating the multi-hot encoded M&R activity indicators. The model performance results after incorporating M&R features are presented in Table 4.

Table 4. Performance of models incorporating baseline and M&R features.

Algorithm	R^2	MAE	RMSE
Linear Regression	0.45	13.66	17.54
Random Forest	0.55	11.94	15.80
XGBoost	**0.56**	**11.80**	**15.68**

Note: Bold values indicate the best performance metric in each column.

The inclusion of M&R variables substantially improved predictive performance across all models. Linear Regression increased from R^2 = 0.24 in Model 1 to R^2 = 0.45 in Model 2, indicating that treatment history contributed considerable explanatory value even within a linear framework. Random Forest improved from R^2 = 0.35 to R^2 = 0.55, while XGBoost improved from R^2 = 0.34 to R^2 = 0.56. These improvements were accompanied by notable reductions in both MAE and RMSE, confirming that M&R history plays a major role in explaining pavement performance change. The strong gain from Model 1 to Model 2 also indicates that treatment information captures important variation that cannot be inferred from baseline pavement and roadway characteristics alone.

4.3. Contribution of Environmental Features (Model 3)

Model 3 further extended Model 2 by incorporating environmental, flood-related, terrain, and deformation variables. The performance results for Model 3 are presented in Table 5.

Table 5. Performance of models incorporating baseline, M&R, and environmental features.

Algorithm	R^2	MAE	RMSE
Linear Regression	0.46	13.53	17.39
Random Forest	0.62	11.13	14.60
XGBoost	**0.65**	**10.63**	**14.02**

Note: Bold values indicate the best performance metric in each column.

Adding environmental variables resulted in further performance gains, particularly for the ensemble-based models. XGBoost achieved the best overall performance in the study (R^2 = 0.65, MAE = 10.63, RMSE = 14.02), while Random Forest also improved substantially, R^2 = 0.62. In contrast, Linear Regression showed only a marginal increase from R^2 = 0.45 to R^2 = 0.46, suggesting that the contribution of environmental variables is largely nonlinear and interaction-driven. These results indicate that climatic, flood-related, terrain, and deformation factors contain meaningful predictive information, but their effects are captured more effectively by nonlinear ensemble methods than by a linear model.

4.4. Comparative Performance Across Modeling Scenarios

Figure 3 presents the comparative model performance across the three modeling scenarios using the coefficient of determination (R^2). The figure shows a consistent increase

in predictive performance from Model 1 to Model 2 and from Model 2 to Model 3 for all three algorithms.

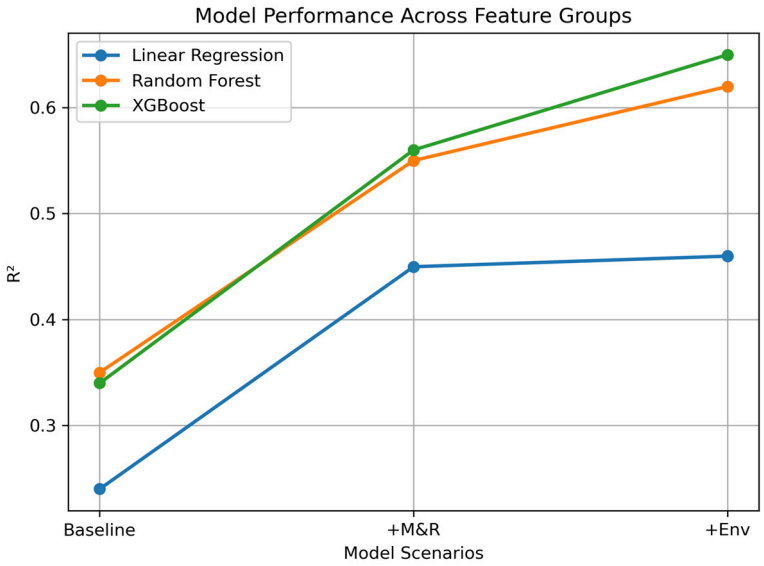


Figure 3. Comparison of model performance across three modeling scenarios based on R^2.

The most substantial improvement occurred between Model 1 and Model 2, demonstrating the strong incremental value of M&R history in explaining pavement performance change. This pattern was especially evident for the nonlinear models, where Random Forest improved by 0.20 (R^2) units and XGBoost improved by 0.22 (R^2) units after adding treatment variables. The transition from Model 2 to Model 3 produced additional gains, particularly for Random Forest and XGBoost, confirming that environmental exposure contributes useful predictive information beyond baseline and treatment data.

Overall, XGBoost achieved the highest predictive performance in the fully integrated scenario, followed by Random Forest, while Linear Regression remained the weakest model across all scenarios. The consistent superiority of the ensemble-based methods indicates that pavement performance change in this dataset is governed by nonlinear and interaction-dependent relationships among baseline condition, M&R history, and environmental variables.

4.5. Learning Curve Analysis

Learning curve analysis was conducted using XGBoost Model 3 to evaluate convergence behavior and assess the impact of training sample size on predictive performance. As shown in Figure 4, validation R^2 increases steadily from approximately 0.54 at smaller training sizes to approximately 0.65 when the full dataset is used, indicating that the model benefits from additional data and effectively captures complex relationships among baseline condition, maintenance history, and environmental exposure. The training R^2 remains consistently high, decreasing slightly from near-perfect fit to approximately 0.95, reflecting improved generalization as more data are incorporated.

The difference between training and validation performance indicates a noticeable generalization gap rather than perfect model convergence. This gap is expected in network-level pavement performance modeling because pavement deterioration is influenced by heterogeneous site conditions, treatment history, environmental exposure, traffic loading, structural capacity, drainage condition, construction quality, and other factors that may not be fully captured in the available dataset. Although the validation R^2 stabilized near 0.65, the training R^2 remained substantially higher, indicating that the XGBoost model

captured complex patterns in the training data but still faced uncertainty when generalizing to unseen segments.

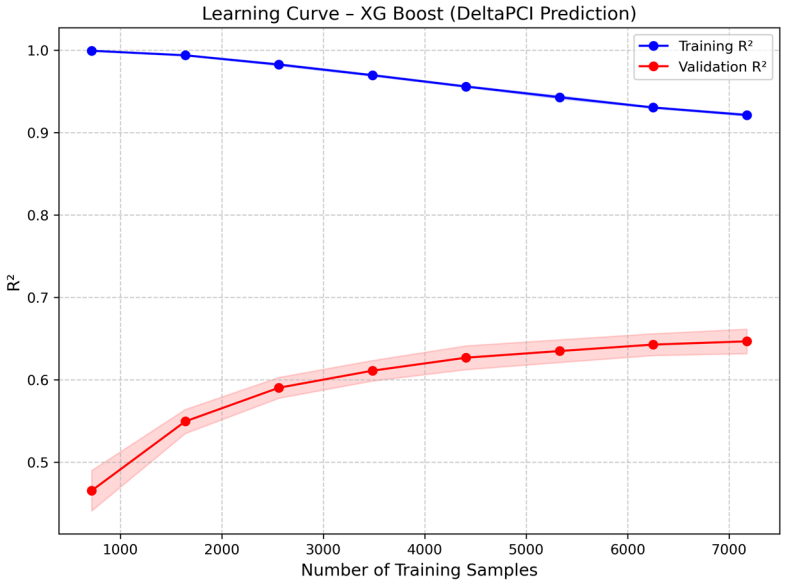


Figure 4. Learning curve for the XGBoost Model 3 showing training and validation R^2 as a function of training sample size.

The validation curve does not fully plateau, suggesting that predictive performance may improve further with additional data or additional explanatory variables. Variables such as pavement age, structural layer thickness, detailed traffic loading, drainage condition, treatment timing, and treatment quality could further improve model generalization if consistently available. Therefore, the observed training-validation gap reflects both model complexity and incomplete system observability in real-world pavement management data. Overall, the learning curve indicates that the XGBoost model provides useful predictive performance while also highlighting the need for additional structural, traffic, and temporal treatment information in future work.

4.6. Model Interpretability Using SHAP Analysis

To better understand the predictions of the final model, SHAP (SHapley Additive exPlanations) analysis was performed using the XGBoost model from Model 3, which had the highest predictive performance. SHAP analysis was used because XGBoost is a nonlinear model, so its prediction process is not as easy to interpret as a Linear Regression model. SHAP values help explain how each input feature contributed to the predicted change in pavement condition, represented by $\Delta PCI = PCI2023 - PCI2019$. Therefore, a higher predicted ΔPCI indicates pavement improvement or less deterioration between 2019 and 2023, while a lower predicted ΔPCI indicates less improvement or greater deterioration. A positive SHAP value means that a feature pushed the model prediction toward a higher ΔPCI, while a negative SHAP value means that a feature pushed the prediction toward a lower ΔPCI.

Figure 5 presents the SHAP summary plot for the XGBoost Model 3. In this plot, each row represents one model feature, and the most important features are shown at the top. Each dot represents one pavement segment in the dataset for that feature. Since the dataset contains 11,214 pavement segments, each row shows how that feature affected predictions across the pavement network. The dots are spread vertically only to reduce overlap and make the plot easier to read.

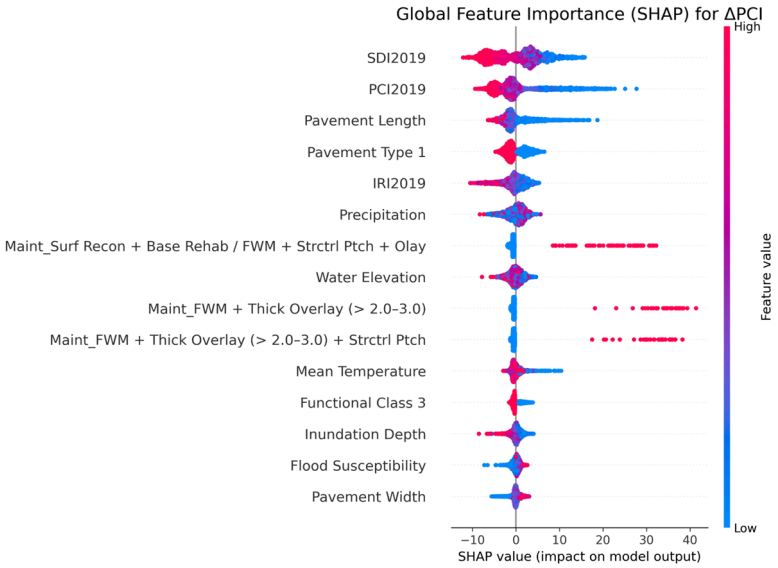


Figure 5. SHAP summary plot showing the top 15 feature contributions to ΔPCI prediction for XGBoost Model 3. Continuous features are interpreted using their original input units, including PCI/SDI indices, pavement length (ft), precipitation (mm), water elevation (ft), mean temperature (°C), and inundation depth (ft). Pavement Type 1 represents asphalt pavement, and Functional Class 3 represents local roads.

The x-axis shows the SHAP value, or how much a feature changed the predicted ΔPCI. Dots on the right side of zero indicate that the feature increased the predicted ΔPCI, while dots on the left side indicate that the feature decreased the predicted ΔPCI. The color shows the actual feature value. For continuous variables, such as SDI2019, PCI2019, pavement length, precipitation, and water elevation, red means higher values and blue mean lower values. For binary variables, such as pavement type, functional class, and M&R treatment indicators, red generally means the feature was present, while blue means it was absent.

The spread of each row also helps explain feature influence. A wide row means that the feature had different levels of impact across many pavement segments and strongly affected predictions. A narrow row means that most SHAP values were close to zero, so the feature had a smaller or more consistent effect. This does not mean the feature was missing. For example, pavement width exists for all segments, but if it did not strongly change the predicted ΔPCI for most segments, its SHAP row appears narrow. Similarly, some M&R rows may appear narrow because most pavement segments did not receive that specific treatment, even though the treatment may still have a strong effect when it was present.

As shown in Figure 5, baseline pavement condition variables were the strongest predictors of pavement performance change. SDI2019 and PCI2019 were the two most influential features, followed by pavement length, pavement type, and IRI2019. This is reasonable because these variables describe the starting condition and basic characteristics of each pavement segment before the 2019–2023 analysis period.

SDI2019 was the highest-ranked feature, showing that initial surface distress condition was very important for predicting future pavement condition change. In practical terms, SDI2019 represents the surface condition of the pavement in 2019. Pavement sections with poorer surface conditions had more opportunities to show improvement if maintenance or rehabilitation were applied. In contrast, pavement sections already in good condition had less room to improve and could show smaller or negative ΔPCI due to normal aging, traffic, and environmental exposure.

PCI2019 was also highly influential because it represents the overall pavement condition at the beginning of the study period. Since ΔPCI is calculated using PCI2019 as the

starting value, the initial PCI strongly affects how much improvement or decline is possible by 2023. For example, a pavement segment with a high PCI in 2019 may remain stable or decline slightly, while a segment with a low PCI in 2019 may show a large positive ΔPCI if it received effective rehabilitation.

Pavement length was also an important feature. In this study, each roadway segment is a GISID-based pavement management unit bounded by an on-street name and from-street/to-street reference points, following the City of Beaumont PMS and GIS inventory structure. Therefore, pavement length represents the length of a management-level roadway unit, not a fixed-length pavement sample. Its importance suggests that the size of the management unit helped explain differences in ΔPCI. Longer segments may include more variation in condition, drainage exposure, intersections, localized distress, and partial maintenance effects, while shorter segments may show more concentrated condition changes. Therefore, pavement length should be interpreted as a management-unit and exposure-related variable, not as a direct cause of pavement improvement or deterioration.

Pavement type and IRI2019 were also important baseline predictors. Pavement type helped the model account for differences between asphalt and other pavement types after considering other variables such as initial condition, roughness, M&R history, and environmental exposure. This does not mean that asphalt pavement always performs better or worse. It only means that pavement type helped explain differences in pavement behavior within the dataset. IRI2019 represents initial pavement roughness and ride quality, where higher roughness can indicate poorer functional condition.

The SHAP summary plot also shows that several M&R and environmental variables contributed to predicted ΔPCI. Environmental variables such as precipitation, water elevation, mean temperature, and inundation depth reflect moisture, flooding, thermal, and hydrologic exposure conditions. M&R variables such as Surf Recon + Base Rehab/FWM + Structural Patch + Overlay, FWM + Thick Overlay (>2.0–3.0), and FWM + Thick Overlay (>2.0–3.0) + Structural Patch were among the most influential treatment-related features. These treatment variables are encoded as a binary indicator variable using Boolean values, meaning that the value of True indicates that the treatment was present for a pavement segment, while the value of False indicates that it was not present.

Overall, the SHAP results show that pavement performance change in Southeast Texas was influenced by the combined effects of initial pavement condition, roadway management-unit characteristics, M&R activity, and environmental exposure. However, baseline condition variables, especially SDI2019 and PCI2019, remained the strongest predictors. This means that the condition of the pavement at the beginning of the analysis period strongly influenced how much the pavement condition changed by 2023.

Finally, SHAP analysis explains model behavior, not direct causation. A high SHAP value means that the model relied strongly on that feature when making predictions. It does not necessarily mean that the feature alone caused pavement improvement or deterioration. Because XGBoost captures nonlinear relationships and interactions, the direction and size of SHAP values may depend on other factors such as baseline condition, pavement type, treatment history, roadway classification, and environmental context.

4.7. Influence of Environmental Variables

Table 6 presents the environmental variables ranked by mean absolute SHAP value, while Figure 6 provides a focused SHAP summary plot for the environmental variables only. In addition, Figure 7 presents environmental SHAP dependence plots to show how the actual values of each environmental variable were associated with changes in SHAP contribution. Together, these results provide both global and variable-specific interpretation. Table 6 identifies the relative importance of each environmental variable, Figure 6 shows the

overall distribution and direction of environmental SHAP values, and Figure 7 illustrates nonlinear relationships between environmental exposure levels and predicted pavement performance change.

Table 6. Environmental variables ranked by Mean |SHAP|.

Rank	Environmental Variable	Mean |SHAP|
1	Precipitation (mm)	1.516
2	Water Elevation (ft)	1.136
3	Mean Temperature (°C)	0.831
4	Inundation Depth (ft)	0.774
5	Flood Susceptibility (dimensionless index)	0.608
6	Ground deformation (mm)	0.545
7	Flood Speed (ft/s)	0.544
8	Topographic Control Index (dimensionless index)	0.340
9	Flood Frequency (count)	0.080

Note: Mean |SHAP| means the average absolute SHAP value of a variable across all pavement segments. It measures how strongly a variable affected the XGBoost Model 3 prediction of ΔPCI, without considering whether the effect was positive or negative. The absolute value is used because positive and negative SHAP values can cancel each other out if a regular mean is used. A higher Mean |SHAP| value means that the variable had a stronger overall influence on model predictions. It does not mean that the variable always increased or always decreased ΔPCI. It only means that the model uses that variable more strongly when making predictions.

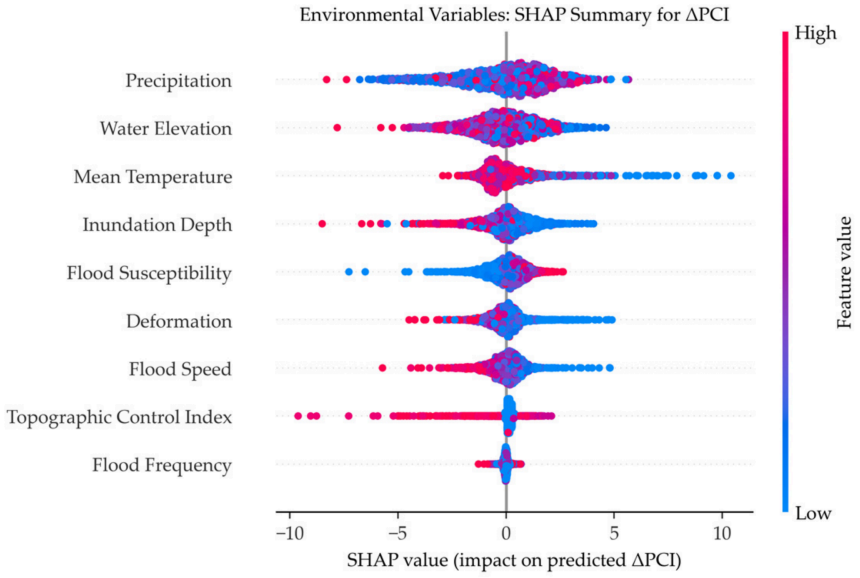


Figure 6. Environmental-only SHAP summary plot for XGBoost Model 3. Each point represents one pavement segment. Red indicates higher feature values and blue indicates lower feature values based on each variable's original input unit, including precipitation (mm), water elevation (ft), mean temperature (°C), inundation depth (ft), flood speed (ft/s), ground deformation (mm), flood frequency (count), and dimensionless flood susceptibility and topographic control index values.

Among the environmental predictors, precipitation was the most influential variable, with a mean absolute SHAP value of 1.516, followed by water elevation (1.136), mean temperature (0.831), and inundation depth (0.774). The remaining environmental variables ranked as flood susceptibility (0.608), ground deformation (0.545), flood speed (0.544), topographic control index (0.340), and flood frequency (0.080). These results indicate that moisture exposure, floodwater-level conditions, thermal exposure, and direct inundation were the most important environmental contributors to ΔPCI prediction in the final XGBoost Model 3.

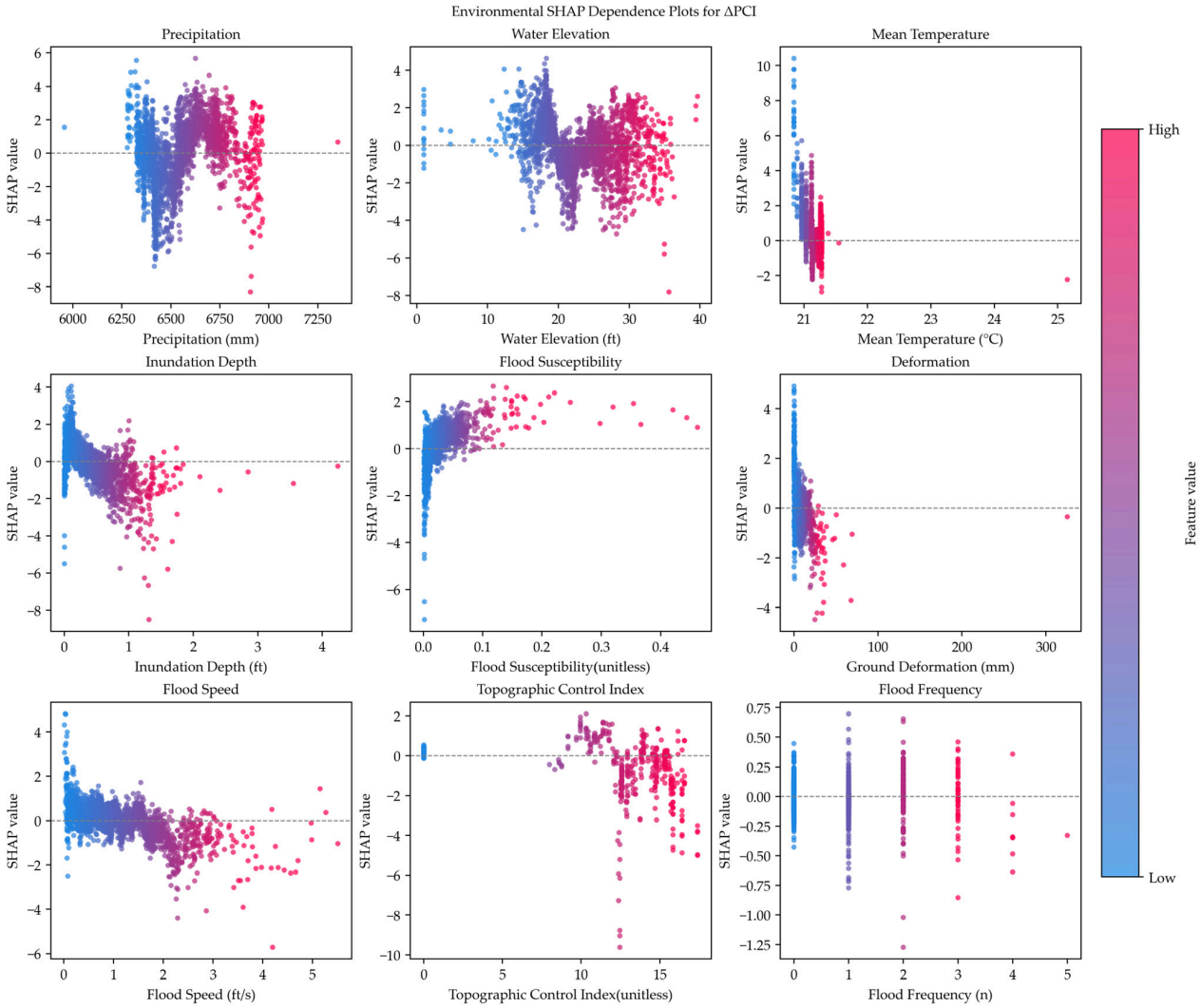


Figure 7. Environmental SHAP dependence plots for XGBoost Model 3.

The SHAP descriptive analysis indicated that the environmental variables did not influence ΔPCI in a uniform manner. Since ΔPCI was defined as PCI2023 − PCI2019, lower ΔPCI values correspond to less improvement or greater deterioration during the study period. In Figure 6, higher values of water elevation, mean temperature, inundation depth, ground deformation, flood speed, topographic control index, and flood frequency were generally associated with lower predicted ΔPCI. This indicates that greater hydrologic, thermal, terrain-related, and deformation stress tended to push predicted pavement performance change downward. These associations are consistent with expected pavement deterioration mechanisms, including moisture infiltration, subgrade weakening, loss of support, thermal aging, hydraulic erosion, and differential settlement in low-lying or flood-prone areas.

The environmental SHAP dependence plots in Figure 7 further show that these relationships were nonlinear and context-dependent. Inundation depth showed one of the clearest negative patterns: as inundation depth increased, SHAP values generally became more negative. This indicates that deeper floodwater over the pavement surface tended to reduce predicted ΔPCI. From an engineering perspective, deeper inundation can promote water infiltration through cracks and joints, weaken base and subgrade layers, reduce bearing capacity, and accelerate pothole formation, cracking, and localized structural failure. For pavement management systems, this suggests that segments exposed to greater inunda-

tion depth should be flagged for closer inspection and may require drainage improvement, structural rehabilitation, or more flood-resilient treatment strategies.

Flood speed also showed a generally negative trend, where higher flood-speed values tended to push predicted ΔPCI downward. This pattern is physically meaningful because faster-moving floodwater can increase hydraulic shear stress, erode shoulder and edge-support material, and weaken pavement support layers through scour and particle displacement. Therefore, flood velocity should be considered alongside flood depth when identifying vulnerable pavement segments. A segment exposed to shallow but fast-moving water may still experience meaningful structural damage due to erosive forces around the pavement edge and supporting layers.

Ground deformation showed that most observations were concentrated near low deformation values, while higher deformation values were generally associated with more negative SHAP contributions. This result is consistent with the role of subsidence or localized ground movement in pavement distress development. Ground deformation can reduce the uniformity of pavement support, induce differential settlement, increase roughness, and accelerate cracking. Although extreme deformation values occurred in relatively few segments, their negative SHAP contributions suggest that localized geotechnical instability can strongly affect predicted pavement performance change.

Topographic control index also displayed a distinct pattern. Many segments had low values, while higher values were grouped in a separate range and were generally associated with negative SHAP contributions. This suggests that terrain conditions that encourage water accumulation, poor drainage, or runoff concentration tended to reduce predicted ΔPCI. From a PMS perspective, topographic control index can be useful for identifying drainage-sensitive locations where water may remain longer after rainfall or flooding. These segments may require targeted drainage improvements, elevation correction, or more durable pavement designs to reduce moisture-related deterioration.

Mean temperature showed a concentrated distribution, with most observations clustered within a narrow range. Higher temperature values generally tended to shift SHAP values downward, although the number of high-temperature observations was limited. This pattern is consistent with the effect of thermal exposure on asphalt materials, where higher temperatures can accelerate binder oxidation, increase brittleness, contribute to rutting, and intensify surface distress progression. Because local temperature variation was relatively narrow, temperature alone may not explain large differences in ΔPCI, but it remains important when combined with moisture, flooding, and baseline pavement condition variables.

Water elevation showed a broad nonlinear relationship with predicted ΔPCI. Water elevation is not the same as water depth on the pavement, but it represents the floodwater surface height measured from a mean sea level. Its effect depends on how high or low the roadway is relative to the floodwater level. Lower road segments may experience deeper surface flooding, while higher road segments may experience little or no direct flooding even when surrounding floodwater levels are high. Therefore, water elevation should be interpreted as an indicator of broader floodwater-level conditions rather than a direct measure of water depth on the pavement. These broader flood conditions may still affect drainage, subgrade saturation, and pavement support.

Precipitation and flood susceptibility showed more mixed patterns. Precipitation had the highest mean absolute SHAP value, indicating a strong overall influence, but its dependence plot showed both positive and negative SHAP contributions across different ranges. Similarly, flood susceptibility often showed positive SHAP values at higher susceptibility levels. These patterns should not be interpreted as evidence that precipitation or flood susceptibility directly improves pavement conditions. Instead, they likely reflect

conditional model-based associations and interactions with other variables, such as baseline condition, pavement type, roadway classification, drainage characteristics, and M&R history. For example, highly flood-susceptible or wetter areas may have received more intensive maintenance, may correspond to higher-priority road classes, or may have different initial pavement conditions. Therefore, the positive SHAP values for these variables likely represent spatial/contextual patterns in the dataset rather than direct causal benefits of environmental exposure.

Flood frequency appeared as vertical bands in the dependence plot because it is a discrete count variable. Higher flood-frequency categories generally showed mixed to negative SHAP contributions, indicating that repeated flood exposure can contribute to reduced predicted ΔPCI, but the effect depends on other segment-level conditions. Repeated flooding can cause cumulative damage by repeatedly saturating pavement layers, weakening subgrade support, and accelerating distress progression over time. However, the limited number of observations at higher flood-frequency levels suggests that interpretation of those categories should be made cautiously.

Overall, the environmental SHAP results show that environmental exposure affects pavement performance through nonlinear and interacting mechanisms rather than through simple one-directional relationships. Variables directly related to flood loading, water movement, terrain-driven drainage, and ground stability, including inundation depth, flood speed, topographic control index, and deformation, generally showed negative associations with predicted ΔPCI. These findings align with known pavement deterioration mechanisms involving moisture infiltration, hydraulic stress, subgrade weakening, erosion of support layers, and differential settlement. For PMS implementation, the results suggest that environmental variables should be integrated with baseline condition and M&R history to identify vulnerable segments, prioritize drainage-sensitive repairs, and support climate-resilient maintenance planning in flood-prone regions. Rather than using environmental exposure variables in isolation, agencies can use them as risk indicators to improve maintenance timing, select more appropriate rehabilitation treatments, and allocate limited resources toward segments where environmental stress is most likely to accelerate deterioration.

4.8. Impact of M&R Activities Based on SHAP Analysis

To further evaluate the role of treatment history, Table 7 ranks the M&R activities by mean absolute SHAP value and application frequency. A focused M&R-only SHAP summary plot is also provided in Figure 8 to show the distribution and direction of treatment-related SHAP values across pavement segments. Table 7 provides exact rankings, treatment counts, percentages, and signed SHAP values when applied, while Figure 8 visually shows how treatment indicators influenced predicted ΔPCI across the test segments. Together, the table and figure help distinguish overall treatment importance, treatment frequency, and directional model behavior.

The M&R data were highly imbalanced. Among the 11,214 matched pavement segments, 1502 segments (13.39%) had a recorded M&R activity during the June 2019–April 2023 period, while 9712 segments (86.61%) had no recorded M&R activity. Therefore, the M&R-related SHAP results should be interpreted as model-based associations with predicted ΔPCI rather than direct causal estimates of treatment effects on pavement condition. The M&R SHAP ranking in Table 7 shows that the most influential treatment based on overall mean absolute SHAP value was Surf Recon + Base Rehab/FWM + Strctrl Ptch + Olay, with a mean absolute SHAP value of 1.454 and a frequency of 366 segments (3.26%). This was followed by FWM + Thick Overlay (>2.0–3.0), with a mean absolute SHAP value of 1.011 and a frequency of 172 segments (1.53%), and FWM + Thick Overlay (>2.0–3.0) +

Strctrl Ptch, with a mean absolute SHAP value of 0.900 and a frequency of 144 segments (1.28%). Additional highly ranked treatments included Edge Mill + Thin Overlay (1.5–2.0) (0.547; 136 segments; 1.21%), ACP Full Depth Reconstruction (0.537; 76 segments; 0.68%), and EM/FWM + Moderate Overlay (2.0–3.0) + Strctrl Ptch (0.419; 157 segments; 1.40%). Overall, the highest-ranked treatments were structurally intensive or overlay-based interventions, indicating that these rehabilitation strategies had the strongest model-based associations with measurable pavement performance change across the full dataset.

Table 7. M&R activities ranked by SHAP importance and application frequency.

Rank	M&R Activity	Count	%	Mean |SHAP|	Mean SHAP (Applied)
1	Surf Recon + Base Rehab/FWM + Strctrl Ptch + Olay	366	3.26	1.454	21.54
2	FWM + Thick Overlay (>2.0–3.0)	172	1.53	1.011	33.83
3	FWM + Thick Overlay (>2.0–3.0) + Strctrl Ptch	144	1.28	0.900	31.10
4	Edge Mill + Thin Overlay (1.5–2.0)	136	1.21	0.547	20.64
5	ACP Full Depth Reconstruction	76	0.68	0.537	30.10
6	EM/FWM + Moderate Overlay (2.0–3.0) + Strctrl Ptch	157	1.40	0.419	13.56
7	EM/FWM + Moderate Overlay (2.0–3.0)	37	0.33	0.189	21.28
8	PCC Slight Pnl Rplcmnt (<10%) + Grind	126	1.12	0.100	−4.38
9	PCC Moderate Pnl Rplcmnt (<20%) + Grind	99	0.88	0.085	−4.75
10	Edge Mill + Thin Overlay (1.5–2.0) + Strctrl Ptch	17	0.15	0.080	23.86
11	Micro Surface/Chip Seal	40	0.36	0.073	10.90
12	Slurry Seal/Seal Coat	9	0.08	0.026	16.69
13	Routine Maintenance	49	0.44	0.010	0.92
14	PCC Localized Rehab + Grind	2	0.02	0.006	−9.27
15	PCC Localized Rehab	42	0.38	0.002	−0.13
16	PCC Jnt Rehab & Crk Seal	13	0.12	0.001	0.10
17	PCC Extensive Pnl Rplcmnt (<33%) + Grind	8	0.07	0.000	0.00
18	Micro Surface/Chip Seal + Strctrl Ptch	4	0.04	0.000	0.00
19	PCC Slight Pnl Rplcmnt (<10%)	5	0.05	0.000	0.00

Note: Count indicates the number of pavement segments in which each M&R activity was recorded during the June 2019 to April 2023 analysis period. Percent represents the corresponding share of the full dataset of 11,214 segments. Mean |SHAP| denotes the average absolute SHAP value of each treatment variable in the XGBoost Model 3 prediction of ΔPCI and represents its overall contribution magnitude, independent of direction. Mean SHAP (Applied) denotes the average signed SHAP value calculated only for segments where the corresponding treatment was present. Positive Mean SHAP (Applied) values indicate that the treatment was associated with higher predicted ΔPCI, whereas negative values indicate association with lower predicted ΔPCI. Abbreviations follow the definitions provided in Table 1 footnote.

The focused M&R SHAP summary plot in Figure 8 supports the tabular ranking by showing that the highest-ranked asphalt rehabilitation treatments produced the widest positive SHAP ranges when present. However, the plot also shows that many treatment indicators had values clustered near zero for most segments, reflecting the sparse and imbalanced nature of the treatment data. This pattern is expected because most roadway segments had no recorded M&R activity during the observation period, and several individual treatments occurred in only a small number of segments.

Although Table 7 ranks M&R activities by mean absolute SHAP value, this metric reflects the overall predictive contribution of each treatment variable across the full dataset, including the large number of segments where a given treatment was not applied. Because M&R variables are binary and highly imbalanced, Figure 9 instead compares treatment frequency with the mean signed SHAP value calculated only for segments where each

treatment was applied. Therefore, Figure 9 should not be interpreted as a replacement ranking for Table 7; rather, it provides a complementary applied-only interpretation showing whether each treatment variable generally pushed predicted ΔPCI upward or downward when present.

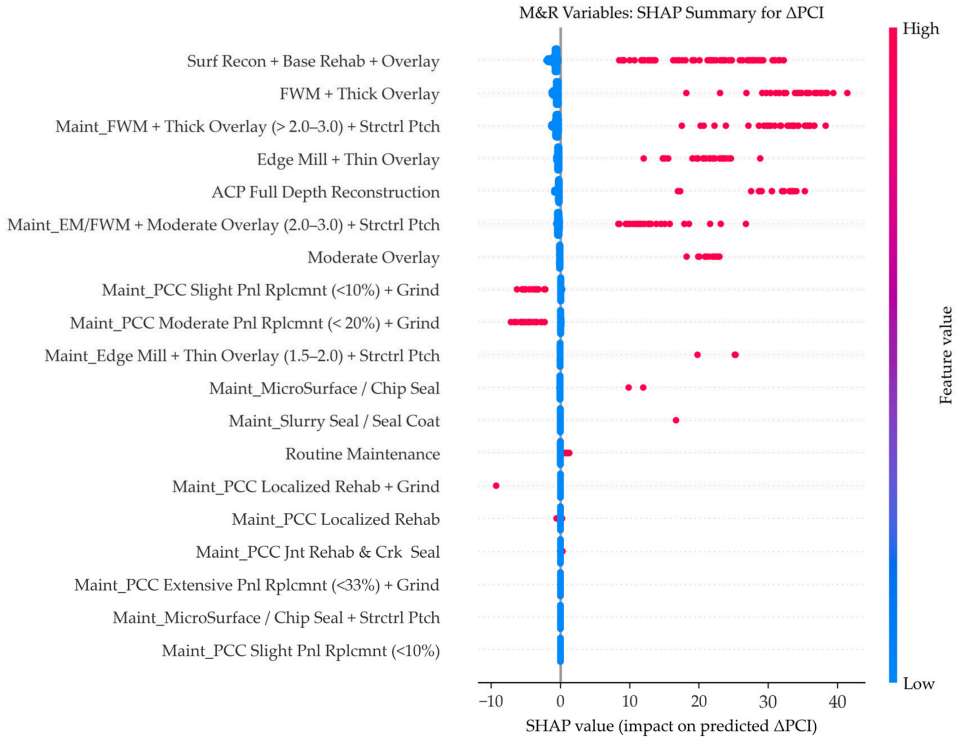


Figure 8. M&R-only SHAP summary plot for XGBoost Model 3. Abbreviations follow the definitions provided in Table 1 footnote.

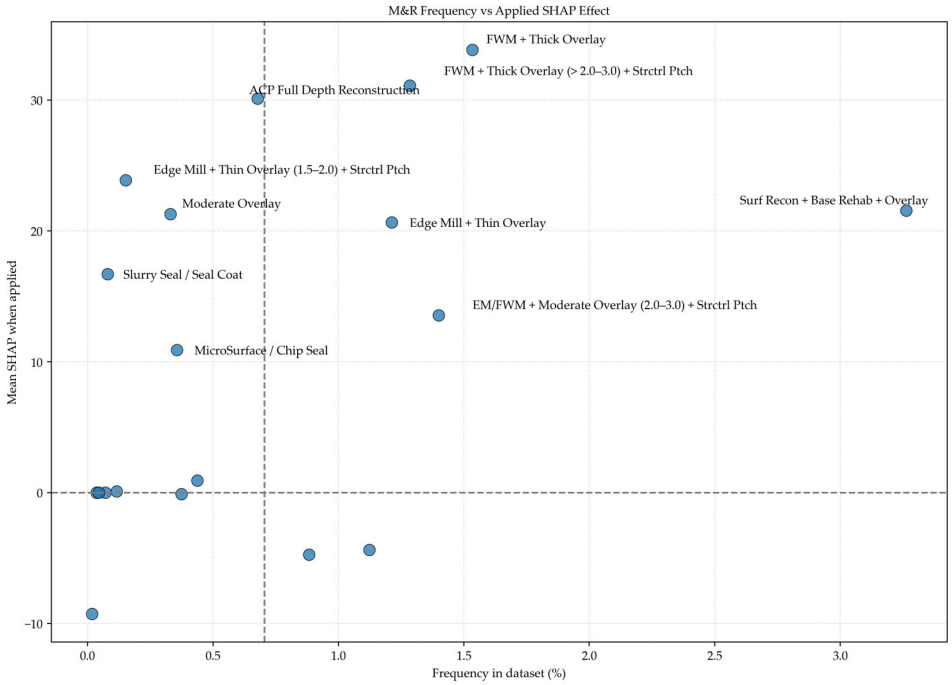


Figure 9. Relationship between M&R application frequency and applied SHAP effect in XGBoost Model 3. Blue points represent individual M&R activities. The dashed vertical line indicates the average treatment frequency across M&R activities, and the dashed horizontal line indicates zero applied SHAP effect. Abbreviations follow the definitions provided in Table 1 footnote.

Figure 9 shows several important patterns for pavement management decision-making. First, the strongest positive applied SHAP effects were associated with structurally intensive or overlay-based treatments, including FWM + Thick Overlay, FWM + Thick Overlay (>2.0–3.0) + Strctrl Ptch, ACP Full Depth Reconstruction, Edge Mill + Thin Overlay, Edge Mill + Thin Overlay (1.5–2.0) + Strctrl Ptch, and Surf Recon + Base Rehab/FWM + Strctrl Ptch + Olay. These treatments generally pushed predicted ΔPCI upward when applied, suggesting that the model associated them with pavement condition improvement or reduced deterioration during the study period. From a PMS perspective, this indicates that structural rehabilitation and thicker overlay strategies may provide stronger measurable condition benefits than routine or minor treatments, especially when applied to segments where deterioration has progressed beyond the preventive-maintenance stage.

Second, Figure 9 shows that treatment frequency and applied SHAP effect do not follow the same pattern. Surf Recon + Base Rehab/FWM + Strctrl Ptch + Olay had the highest application frequency and a positive applied SHAP value, indicating that it was both commonly used and associated with higher predicted ΔPCI when present. FWM + Thick Overlay and FWM + Thick Overlay (>2.0–3.0) + Strctrl Ptch also showed high positive applied SHAP values at moderate application frequencies, suggesting that overlay-based rehabilitation activities were important contributors to predicted pavement improvement when applied. In contrast, some lower-frequency treatments, such as Edge Mill + Thin Overlay (1.5–2.0) + Strctrl Ptch and Slurry Seal/Seal Coat, also showed positive applied SHAP values despite being applied to relatively few segments. These results suggest that low-frequency treatments should not automatically be considered unimportant in PMS planning; rather, they may be effective under specific pavement conditions or treatment-selection contexts. However, because these treatments have smaller sample sizes, their interpretation should remain cautious.

Third, several localized or PCC-related treatments showed near-zero or negative applied SHAP values. These negative applied SHAP values should not be interpreted as evidence that the treatments caused pavement deterioration. More likely, they reflect treatment selection bias and initial-condition effects, where corrective or localized repairs were applied to pavement segments that were already in poor condition, structurally deficient, or subject to greater deterioration pressure. In PMS practice, this highlights the importance of combining treatment history with baseline condition, pavement type, and distress severity before interpreting treatment performance. A treatment applied to a severely deteriorated segment may still be necessary and beneficial, even if the observed ΔPCI over the study period remains low or negative.

Figure 9 can therefore be interpreted using a frequency–applied-effect framework. Treatments with relatively high frequency and positive applied SHAP values represent commonly recorded rehabilitation activities that generally pushed predicted ΔPCI upward when applied. These treatments may be especially relevant for PMS prioritization because they combine broader network use with positive model-based performance association. Low-frequency treatments with positive applied SHAP values may indicate specialized interventions that were associated with higher predicted ΔPCI when applied, but they should be interpreted cautiously because of limited sample size. Treatments with near-zero applied SHAP values suggest limited short-term influence on predicted ΔPCI within the observation window, while treatments with negative applied SHAP values may reflect corrective applications on already deteriorated segments rather than harmful treatment performance.

Overall, the combined interpretation of Table 7 and Figure 9 provides a more useful basis for PMS decision-making than either metric alone. Mean |SHAP| identifies which M&R variables were most important to the XGBoost model across the entire network, while Mean SHAP (Applied) shows how the model interpreted each treatment when it was

present. This distinction is important for maintenance prioritization because agencies need to know both which treatments strongly influence network-level prediction and which treatments are associated with positive condition change when applied. The results suggest that PMS workflows should account for treatment intensity, treatment frequency, initial pavement condition, treatment objective, sample size, and treatment-selection context rather than relying only on treatment counts or overall feature importance. Such interpretation can support more transparent rehabilitation planning, help justify the use of structural treatments on high-need segments, and improve the allocation of limited maintenance resources across the pavement network.

4.9. Key Findings

The main findings of this study can be summarized as follows:

- Baseline pavement and roadway feature alone had limited explanatory power. In Model 1, the best-performing baseline model achieved $R^2 = 0.35$, showing that baseline variables explained only about 35% of the variation in ΔPCI.
- M&R history provided the largest improvement in prediction. After adding the 19 M&R activity variables, the best model achieved $R^2 = 0.56$, a gain of 0.21 R^2 units, indicating that treatment history was the single most important additional contributor to explained variance and can explained 21% of the variation in ΔPCI.
- Environmental variables added further value, but less than M&R. In Model 3, the best-performing baseline model achieved $R^2 = 0.65$, showing that environmental and flood-related factors can explained 9% of the variation in ΔPCI beyond baseline and M&R information.
- XGBoost achieved the highest predictive performance in the fully integrated scenario ($R^2 = 0.65$, MAE = 10.63, and RMSE = 14.02), outperforming both Random Forest and Linear Regression. This confirms that nonlinear ensemble models were better suited to capturing the combined effects of pavement condition, M&R history, and environmental exposure.
- SHAP analysis showed that baseline conditions remained dominant, while M&R and environmental factors added meaningful explanation. SDI2019 and PCI2019 were the most influential overall predictors. Among M&R variables, the most important were Surf Recon + Base Rehab/FWM + Strctrl Ptch + Olay, FWM + Thick Overlay (>2.0–3.0), and FWM + Thick Overlay (>2.0–3.0) + Strctrl Ptch. Among environmental variables, precipitation, water elevation, mean temperature, and inundation depth were the strongest contributors.
- Environmental SHAP dependence plots showed that environmental effects were nonlinear and context-dependent. Variables directly related to flood loading, terrain-driven water accumulation, and ground instability, including inundation depth, flood speed, topographic control index, and deformation, generally pushed predicted ΔPCI downward. Precipitation and flood susceptibility showed mixed associations, likely reflecting interactions with baseline condition, pavement type, roadway classification, M&R history, and local spatial context.
- The applied-only M&R SHAP analysis showed that several structural and overlay-based treatments generally pushed predicted ΔPCI upward when present. However, negative applied SHAP values for some localized or PCC-related treatments should not be interpreted as harmful treatment effects; rather, they likely reflect treatment selection bias, poorer initial pavement condition, or corrective treatments applied to already distressed segments.

5. Discussion

5.1. Interpretation of Model Performance Improvements

The comparative modeling results indicate that pavement performance change cannot be explained adequately by baseline condition indicators alone. Although baseline descriptors remain essential for network-level assessment, the observed improvement after adding treatment and environmental variables suggests that pavement performance evolves through a combination of prior condition, intervention history, and external stressors rather than through static condition measures alone.

The largest improvement occurred when M&R history was added in Model 2, indicating that treatment history provides substantial explanatory value beyond baseline pavement characteristics. Additional improvement was observed in Model 3 after environmental variables were included, particularly for the ensemble-based models. This pattern suggests that environmental effects are largely nonlinear and interaction-driven, which explains why the ensemble-based models outperformed the linear model. Overall, the final predictive performance indicates that integrating baseline condition, treatment history, and environmental exposure provides the most informative predictive framework for ΔPCI in the study area. This integrated approach represents a methodological advancement over conventional PMS deterioration models, which typically rely on separate univariate or bivariate regression curves for individual distress types without simultaneously accounting for the interacting effects of maintenance history and environmental exposure.

5.2. Insights from M&R Activities and Treatment Frequency

The SHAP-based treatment analysis shows that M&R effects were not uniform across activities. Based on overall mean absolute SHAP values, structurally intensive and overlay-based treatments exhibited the strongest contribution to predicted pavement performance change. These treatments included Surf Recon + Base Rehab/FWM + Strctrl Ptch + Olay, FWM + Thick Overlay (>2.0–3.0), FWM + Thick Overlay (>2.0–3.0) + Strctrl Ptch, Edge Mill + Thin Overlay (1.5–2.0), and ACP Full Depth Reconstruction. This pattern suggests that the model was particularly responsive to rehabilitation strategies involving greater structural or surface improvement.

The applied-only SHAP analysis provides an additional interpretation by examining the mean signed SHAP value only for segments where each treatment was present. This distinction is important because M&R variables were binary and highly imbalanced, with most segments having no recorded treatment. Therefore, mean absolute SHAP values describe overall predictive importance across the full dataset, while mean SHAP when applied describes the direction of model contribution among treated segments only.

The frequency–applied-effect comparison showed that treatment frequency alone did not determine treatment-related model behavior. Some treatments were both relatively common and associated with positive applied SHAP values, indicating that they were widely used and generally pushed predicted ΔPCI upward when present. Other treatments were less frequent but still showed positive applied SHAP values, suggesting that specialized or less common interventions may still be relevant under specific pavement conditions. In contrast, some localized or PCC-related activities showed near-zero or negative applied SHAP values. These negative values should not be interpreted as evidence that the treatments caused deterioration. Instead, they likely reflect treatment selection bias, where corrective or localized repairs were applied to segments already in poor condition, structurally deficient, or under greater deterioration pressure.

Overall, these findings indicate that M&R interpretation should consider both overall predictive importance and applied-only SHAP direction. For PMS applications, this means treatment prioritization should not be based only on how often a treatment is used or how

high it ranks globally, but also on treatment intensity, pavement condition before treatment, treatment objective, and the context in which the treatment was applied.

5.3. Role of Environmental and Flood-Related Factors

The environmental SHAP analysis indicates that climatic, hydrologic, terrain, and deformation variables contributed meaningfully to pavement performance prediction, although their influence remained lower than that of the strongest baseline pavement variables. Overall, precipitation, water elevation, mean temperature, and inundation depth emerged as the most important environmental contributors, highlighting the importance of flood-related and climate-related stress in the study area.

The environmental SHAP dependence plots further showed that these effects were nonlinear and context-dependent. Variables directly associated with flood loading, drainage behavior, and ground stability, including inundation depth, flood speed, topographic control index, and deformation, generally showed negative associations with predicted ΔPCI. These patterns are physically consistent with known pavement deterioration mechanisms in flood-prone regions. Greater inundation depth can increase moisture infiltration, weaken base and subgrade layers, and reduce bearing capacity. Higher flood speed can increase hydraulic shear stress, erode shoulder and edge support, and weaken pavement support layers. Higher topographic control index values may indicate locations where runoff accumulates or water remains longer, increasing moisture-related deterioration risk. Ground deformation can reduce uniform support beneath the pavement structure and contribute to differential settlement, roughness progression, and cracking.

The dependence plots also showed mixed or positive associations for precipitation and flood susceptibility. These results should not be interpreted as evidence that precipitation or flood susceptibility directly improves pavement conditions. Instead, they likely reflect conditional model-based associations and interactions with baseline pavement condition, M&R history, pavement type, roadway classification, local drainage, and spatial context. For example, segments in wetter or more flood-susceptible areas may have received more maintenance attention or may correspond to higher-priority roadway classes. Therefore, these variables should be interpreted as contextual risk indicators rather than direct causal drivers of improvement.

The fact that Random Forest and XGBoost benefited more than Linear Regression from the inclusion of environmental variables supports the conclusion that environmental effects are largely nonlinear and interaction-dependent. This suggests that environmental stressors influence pavement performance through coupled relationships with baseline condition and treatment history rather than through simple independent linear effects.

5.4. Implications for Pavement Management Practice

The findings have several practical implications for sustainable, network-level pavement management. The limited performance of the baseline models indicates that reliance on condition indicators alone may lead to incomplete projections of future pavement behavior. Although PCI, IRI, and related baseline variables remain essential descriptors, they do not fully capture the combined effects of treatment history and environmental exposure. Therefore, the proposed framework provides practical value by integrating pavement condition, M&R history, and environmental exposure into a single predictive workflow. Transportation agencies can use this approach to update pavement management systems after each inspection cycle, estimate segment-level ΔPCI, and identify roadway segments with higher risk of deterioration.

The SHAP-based treatment and environmental analyses further improve practical usability by showing which factors contribute most strongly to predicted pavement perfor-

mance change. In an agency workflow, the model could be applied after each biennial or annual inspection cycle by linking updated PCI and M&R records to the environmental and terrain data described in Section 3.2.4, then generating segment-level ΔPCI predictions for the full network. Segments with predicted ΔPCI below a defined threshold—for example, a projected decline of 10 or more PCI points—could be flagged for priority review. SHAP outputs would then allow field engineers to determine whether the predicted deterioration is primarily driven by poor baseline condition, absence of recent treatment, or elevated flood and climate exposure, supporting a more targeted and defensible maintenance prioritization process. This workflow is compatible with widely used PMS platforms such as MicroPAVER and StreetSaver, where ΔPCI predictions and SHAP-ranked risk factors could supplement existing deterioration curves and treatment cost-effectiveness analyses. Overall, this approach can assist agencies in shifting from reactive repair toward proactive, data-driven, and climate-informed resource allocation.

The environmental dependence analysis and applied-only M&R SHAP interpretation further strengthen this PMS workflow. Environmental dependence plots can help agencies identify whether predicted deterioration is associated with specific exposure mechanisms, such as deeper inundation, faster floodwater movement, terrain-driven water accumulation, or ground deformation. These outputs can support risk-screening for drainage-sensitive segments and help prioritize post-flood inspection or climate-resilient rehabilitation. Similarly, the applied-only M&R SHAP results help agencies interpret how treatments behaved when they were present, avoiding bias from the large number of untreated segments. Together, these explainable ML outputs can help distinguish network-level feature importance, treatment-specific applied effects, and environmentally sensitive pavement locations.

From a sustainability perspective, improved ΔPCI prediction can support more efficient use of materials, labor, and financial resources by helping agencies target interventions where they are most needed. In flood-vulnerable regions such as Southeast Texas, integrating environmental exposure into pavement performance modeling can also support climate-resilient maintenance planning. Overall, the framework can assist agencies in shifting from reactive repair toward more proactive, data-driven, and sustainable pavement management.

5.5. Limitations and Future Research Directions

Although this study provides a useful machine-learning framework for predicting pavement performance changes, several limitations should be acknowledged. First, the available City of Beaumont dataset did not include pavement age, structural layer thickness, detailed traffic loading, drainage condition, or construction quality information for all matched segments. These variables are known to influence pavement deterioration and may partly explain the limited predictive capability of the baseline models and the remaining generalization gap observed in the learning curve. Future studies should incorporate these variables when consistently available to improve model robustness and engineering interpretability.

Second, M&R activities were encoded as binary indicators because the available dataset identified whether a treatment type was recorded during the June 2019–April 2023 observation period, but did not provide consistently available treatment timing, sequencing, treatment age, or construction quality information for all matched segments. As a result, the model could evaluate the association between treatment categories and ΔPCI but could not explicitly capture how long ago a treatment was applied or how treatment order influenced pavement performance. Future work should incorporate treatment chronology, treatment

age, and post-treatment exposure period to better evaluate treatment-related performance associations and causal effects.

Third, the model evaluation used random train-test splitting and cross-validation within the available dataset. While this approach provides a useful estimate of predictive performance, nearby roadway segments may share similar traffic, environmental, and maintenance characteristics, which can introduce spatial autocorrelation. Future studies should consider spatial cross-validation or location-based holdout testing to evaluate model transferability across different parts of the network.

Finally, SHAP analysis was used to interpret feature contributions in the XGBoost Model 3, but SHAP values should be interpreted as model-based associations rather than causal effects. Therefore, the M&R and environmental interpretations in this study should not be viewed as direct estimates of treatment effectiveness or environmental causality. Future research could combine machine learning with causal inference, controlled before-and-after treatment analysis, or mechanistic pavement deterioration models to better separate predictive association from causal impact.

6. Conclusions

This study developed a machine learning-based comparative framework to predict pavement performance change (ΔPCI) for 11,214 matched pavement segments in Southeast Texas from 2019 to 2023. Three nested modeling scenarios were used to evaluate the incremental contribution of baseline pavement and roadway variables, M&R history, and environmental exposure. The results showed that baseline variables alone had limited predictive power, with the best baseline model reaching $R^2 = 0.35$. Adding M&R history produced the largest improvement, increasing model performance to $R^2 = 0.56$, while adding environmental variables provided further gains, raising XGBoost performance to $R^2 = 0.65$. These results demonstrate that pavement performance change is better predicted when treatment history and environmental exposure are integrated with traditional pavement condition indicators. Among the evaluated models, XGBoost achieved the best overall performance ($R^2 = 0.65$, MAE = 10.63, RMSE = 14.02), confirming that pavement performance change is better captured through nonlinear models than through Linear Regression alone.

SHAP analysis identified SDI2019 and PCI2019 as the strongest overall predictors, while selected M&R and environmental variables also contributed meaningfully. Among the M&R variables, structurally intensive and overlay-based treatments such as Surf Recon + Base Rehab/FWM + Strctrl Ptch + Olay, FWM + Thick Overlay (>2.0–3.0), and FWM + Thick Overlay (>2.0–3.0) + Strctrl Ptch showed the highest overall mean absolute SHAP importance. The applied-only M&R SHAP analysis further showed that several structural and overlay-based treatments generally pushed predicted ΔPCI upward when present, while negative applied SHAP values for some localized or PCC-related treatments likely reflected treatment selection bias and poorer initial pavement condition rather than direct negative treatment effects. Among environmental variables, precipitation, water elevation, mean temperature, and inundation depth were the strongest contributors. Environmental SHAP dependence plots showed that these effects were nonlinear and context-dependent, with inundation depth, flood speed, topographic control index, and deformation generally associated with lower predicted ΔPCI.

Overall, the findings show that baseline pavement condition provides the foundation for prediction, M&R history contributes the largest incremental explanatory value, and environmental exposure provides additional improvement, particularly for ensemble-based models. From a practical and sustainability perspective, integrating treatment history and environmental exposure into pavement management workflows can improve

forecasting, support more efficient allocation of maintenance resources, and assist agencies in prioritizing climate-resilient interventions in flood-prone regions. This is especially important for Southeast Texas, where heavy rainfall, flooding, and low-lying terrain can increase long-term pavement vulnerability.

However, even the best-performing model explained 65% of the variance in ΔPCI, leaving approximately 35% unexplained. This remaining variability suggests that pavement performance is also influenced by additional factors not captured in the current dataset, such as traffic loading, pavement age, structural layer thickness, drainage condition, and treatment sequencing. Incorporating these variables in future research, along with treatment timing and spatial validation methods, may help improve model generalization and further strengthen climate-informed and sustainable pavement performance prediction.

Author Contributions: Conceptualization, S.B. and N.B.; methodology, S.B.; software, S.B.; validation, S.B., M.F., A.S.N., M.K. and H.H.A.; formal analysis, S.B.; investigation, S.B.; resources, N.B.; data curation, S.B., M.F., A.S.N. and M.K.; writing—original draft preparation, S.B.; writing—review and editing, N.B., M.F., A.S.N., M.K. and H.H.A.; visualization, S.B.; supervision, N.B., M.F. and A.S.N.; project administration, N.B.; funding acquisition, N.B. All authors have read and agreed to the published version of the manuscript.

Funding: This research was funded by U.S. Department of Energy, Office of Science, Biological and Environmental Research Program under Award Number DE-SC0023216, and the Center for Resiliency (CfR) at Lamar University.

Institutional Review Board Statement: Not applicable.

Informed Consent Statement: Not applicable.

Data Availability Statement: The datasets analyzed in this study are publicly available and described in Hariri Asli et al. [24]. Processed datasets generated during the current study are available from the corresponding author upon reasonable request.

Conflicts of Interest: The authors declare no conflicts of interest.

Abbreviations

The following abbreviations are used in this manuscript:

PCI	Pavement Condition Index
IRI	International Roughness Index
SI	Structural Index
SDI	Surface Distress Index
M&R	Maintenance and Rehabilitation
ML	Machine Learning
PMS	Pavement Management System
RMSE	Root Mean Square Error
MAE	Mean Absolute Error
R^2	Coefficient of Determination
SHAP	SHapley Additive exPlanations
XGBoost	Extreme Gradient Boosting
GIS	Geographic Information System
PRISM	Parameter–Elevation Regressions on Independent Slopes Model

References

1. Baladi, G.Y.; Dawson, T.; Musunuru, G.; Prohaska, M.; Thomas, K. *Pavement Performance Measures and Forecasting and the Effects of Maintenance and Rehabilitation Strategy on Treatment Effectiveness*; Federal Highway Administration: McLean, VA, USA, 2017.
2. Putra, D.A.; Suprapto, M. Assessment of the road based on PCI and IRI roadroid measurement. In *Proceedings of the MATEC Web of Conferences*; EDP Sciences: Les Ulis, France, 2018.

3. Gharaibeh, N.G.; Narciso, P.; Cha, Y.; Oh, J.; Menendez, J.R.; Dessouky, S.; Wimsatt, A. *A Methodology to Support the Development of 4-Year Pavement Management Plan*; United States Department of Transportation: Washington, DC, USA, 2014.
4. Sarsam, S.I. Pavement maintenance management system: A review. *Trends Transp. Eng. Appl.* **2016**, *3*, 19–30.
5. Shamsabadi, S.S.; Tari, Y.S.H.; Birken, R.; Wang, M. Deterioration forecasting in flexible pavements due to floods and snow storms. In Proceedings of the EWSHM-7th European Workshop on Structural Health Monitoring, Nantes, France, 8–11 July 2014.
6. Alaswadko, N.; Hassan, R.; Meyer, D.; Mohammed, B. Modelling roughness progression of sealed granular pavements: A new approach. *Int. J. Pavement Eng.* **2019**, *20*, 222–232.
7. Mills, B.N.; Tighe, S.L.; Andrey, J.; Smith, J.T.; Parm, S.; Huen, K. *Road Well-Traveled: Implications of Climate Change for Pavement Infrastructure in Southern Canada*; Transportation Association of Canada (TAC): Ottawa, ON, Canada, 2007.
8. Zeiada, W.; Hamad, K.; Omar, M.; Underwood, B.S.; Khalil, M.A.; Karzad, A.S. Investigation and modelling of asphalt pavement performance in cold regions. *Int. J. Pavement Eng.* **2019**, *20*, 986–997.
9. Lu, D.; Tighe, S.L.; Xie, W.-C. Impact of flood hazards on pavement performance. *Int. J. Pavement Eng.* **2020**, *21*, 746–752.
10. Sultana, M.; Chai, G.; Martin, T.; Chowdhury, S. Modeling the postflood short-term behavior of flexible pavements. *J. Transp. Eng.* **2016**, *142*, 04016042. [CrossRef]
11. Abdollahi, S.F.; Kutay, M.E.; Lanotte, M. UPDAPS-Flood: A mechanistic-empirical flexible pavement analysis tool to evaluate the effect of flooding events on flexible pavement performance. *Int. J. Pavement Eng.* **2024**, *25*, 2387743. [CrossRef]
12. Conoscenti, C.; Rotigliano, E. Predicting gully occurrence at watershed scale: Comparing topographic indices and multivariate statistical models. *Geomorphology* **2020**, *359*, 107123. [CrossRef]
13. Bakhrel, U. *Identifying Urban Pluvial Nuisance Flooding Hotspots Using the Topographic Control Index and Remote Sensing Radar Images*; Lamar University-Beaumont: Beaumont, TX, USA, 2024.
14. Khorrami, M.; Alizadeh, B.; Ghasemi Tousi, E.; Shakerian, M.; Maghsoudi, Y.; Rahgozar, P. How groundwater level fluctuations and geotechnical properties lead to asymmetric subsidence: A PSInSAR analysis of land deformation over a transit corridor in the Los Angeles metropolitan area. *Remote Sens.* **2019**, *11*, 377. [CrossRef]
15. Nur, A.S.; Nam, B.H.; Choi, S.; Kim, Y.J. Monitoring of ground subsidence using PS-InSAR technique in the Southeast Texas (SETX) Region. *Int. J. Geo-Eng.* **2024**, *15*, 13. [CrossRef]
16. Asli, H.H. *Optimizing Pavement Performance Prediction Using Data-Driven Methods: Integrating Structural, Environmental, Maintenance, and Flood-Related Factors in Beaumont, Texas*; Lamar University-Beaumont: Beaumont, TX, USA, 2025.
17. Tamagusko, T.; Correia, M.G.; Ferreira, A. Machine learning applications in road pavement management: A review, challenges and future directions. *Infrastructures* **2024**, *9*, 213. [CrossRef]
18. Radwan, M.M.; Zahran, E.M.; Dawoud, O.; Abunada, Z.; Mousa, A. Comparative analysis of asphalt pavement condition prediction models. *Sustainability* **2025**, *17*, 109. [CrossRef]
19. Gong, H.; Sun, Y.; Shu, X.; Huang, B. Use of random forests regression for predicting IRI of asphalt pavements. *Constr. Build. Mater.* **2018**, *189*, 890–897. [CrossRef]
20. Ali, A.A.; Milad, A.; Hussein, A.; Yusoff, N.I.M.; Heneash, U. Predicting pavement condition index based on the utilization of machine learning techniques: A case study. *J. Road Eng.* **2023**, *3*, 266–278. [CrossRef]
21. Haddad, A.J.; Chehab, G.R.; Saad, G.A. The use of deep neural networks for developing generic pavement rutting predictive models. *Int. J. Pavement Eng.* **2022**, *23*, 4260–4276.
22. Buss, A.; Claypool, B.; Bektas, F.; Fathy-Abdelaty, A. *Effectiveness of Pavement Preservation Techniques*; National Academies of Sciences, Engineering, and Medicine: Washington, DC, USA, 2019.
23. Al-Mansour, A.; Lee, K.-W.W.; Al-Qaili, A.H. Prediction of pavement maintenance performance using an expert system. *Appl. Sci.* **2022**, *12*, 4802. [CrossRef]
24. Asli, H.H.; Brake, N.; Feizbahr, M.; Bakhrel, U.; Arbabkhah, H.; Jahangir, M.S. Pavement condition and climatic data in southeast Texas: A dataset for evaluating flood impacts on pavement performance. *Data Brief* **2025**, *62*, 111914. [CrossRef]
25. Hong, F.; Wu, H.; Li, J.; Paul, E. Evaluation of flood-vulnerable pavement network in support of resilience in pavement system management. *Transp. Res. Rec.* **2023**, *2677*, 474–482. [CrossRef]
26. Vallès-Vallès, D.; Torres-Machi, C. Deterioration of flexible pavements induced by flooding: Case study using stochastic Monte Carlo simulations in discrete-time Markov chains. *J. Infrastruct. Syst.* **2023**, *29*, 05022009. [CrossRef]
27. Feizbahr, M.; Brake, N.; Arbabkhah, H.; Asli, H.H.; Woods, K. Flood Susceptibility Mapping Using Machine Learning and Geospatial-Sentinel-1 SAR Integration for Enhanced Early Warning Systems. *Remote Sens.* **2025**, *17*, 3471. [CrossRef]
28. Bakhrel, U.; Brake, N.; Feizbahr, M.; Kim, Y.J.; Asli, H.H.; Haselbach, L.; Macon, S.J. Identifying Urban Pluvial Frequency Flooding Hotspots Using the Topographic Control Index and Remote Sensing Radar Images for Early Warning Systems. *Water* **2025**, *17*, 3500. [CrossRef]
29. Wang, Y. Performance of Concrete Crushed-stone Asphalt Overlay Pavement Based on Decision Tree Model. *Prog. Eng. Sci.* **2026**, *3*, 100215. [CrossRef]

30. Ibironke, A.; Dhakal, U.; Bhusal, S.; Wu, X.; Kim, Y.J.; Lai, F.; Toosi, G. Three-dimensional Drainage Infrastructure Modeling for Flood Vulnerability in Southeast Texas. *Photogramm. Eng. Remote Sens.* 2026, *in press*. [CrossRef]
31. Yang, Q.; Tian, W.; Dai, X. Machine Learning-Based Highway Pavement Performance Prediction in Xinjiang. *Infrastructures* **2025**, *10*, 189. [CrossRef]

Disclaimer/Publisher's Note: The statements, opinions and data contained in all publications are solely those of the individual author(s) and contributor(s) and not of MDPI and/or the editor(s). MDPI and/or the editor(s) disclaim responsibility for any injury to people or property resulting from any ideas, methods, instructions or products referred to in the content.